Journal of Magnetic Resonance **141,** 347–354 (1999)
Article ID jmre.1999.1910, available online at http://www.idealibrary.com on IDEAL®

# $^1$H DNP at 1.4 T of Water Doped with a Triarylmethyl-Based Radical

Robert A. Wind*,[1] and Jan-Henrik Ardenkjær-Larsen†

*Pacific Northwest National Laboratory, P.O. Box 999, MS K8-98, Richland, Washington 99352; and
†Nycomed Innovation AB, Ideon Malmö, S-20512 Malmö, Sweden

Received June 16, 1999; revised August 10, 1999

**Recently a triarylmethyl-based (TAM) radical has been developed for research in biological and other aqueous systems, and in low magnetic fields, 10 mT or less, large $^1$H dynamic nuclear polarization (DNP) enhancements have been reported. In this paper the DNP properties of this radical have been investigated in a considerably larger field of 1.4 T, corresponding to proton and electron Larmor frequencies of 60 MHz and 40 GHz, respectively. To avoid excessive microwave heating of the sample, an existing DNP NMR probe was modified with a screening coil, wound around the sample capillary and with its axis perpendicular to the electric component of the microwave field. It was found that with this probe the temperature increase in the sample after 4 s of microwave irradiation with an incident power of 10 W was only 16°C. For the investigations, 10 mM of the TAM radical was dissolved in deionized, but not degassed, water and put into a 1-mm i.d. and 6-mm long capillary tube. At 26°C the following results were obtained: (I) The relaxivity of the radical is 0.07 $(\text{mMs})^{-1}$, in accordance with the value extrapolated from low-field results; (II) The leakage factor is 0.63, the saturation factor at maximum power is 0.85, and the coupling factor is −0.0187. It is shown that these results agree very well with an analysis where the electron–dipolar interactions are the dominant DNP mechanism, and where the relaxation transitions resulting from these interactions are governed by translational diffusion of the water molecules. Finally, the possibilities of combining DNP with magnetic resonance microscopy (MRM) are discussed. It is shown that at 26°C the overall DNP-enhanced proton polarization should become maximal in an external field of 0.3 T and become comparable to the thermal equilibrium polarization in a field of 30 T, considerably larger than the largest high-resolution magnet available to date. It is concluded that DNP MRM in this field, which corresponds to a standard microwave frequency of 9 GHz, has the potential to significantly increase the sensitivity in NMR and MRI experiments of small aqueous samples doped with the TAM radical.** 

*Key Words:* **DNP; Overhauser effect; TAM radical; microwave heating; MR microscopy.**

Inserting paramagnetic labels into biological systems can be used in electron paramagnetic resonance imaging (EPRI) and Overhauser magnetic resonance imaging (OMRI) to determine directly and indirectly the spatial distribution of the label and to measure the local concentration of dissolved molecular oxygen (*1–5*). In OMRI, the NMR signal of the water protons is enhanced by dynamic nuclear polarization (DNP) of the Overhauser type (*6–11*). In principle this can result in a large enhancement of the nuclear polarization, maximal on the order of the ratio of the electron and nuclear gyromagnetic ratios. Especially promising for this type of applications is a radical that has been developed recently, which is based on the triarylmethyl (TAM) molecule (*4, 5, 12*). It has been found that this radical is stable in biological objects (*5*), has excellent water solubility, and has a reasonably large relaxivity (*12*). Also, the TAM radical has several advantages over the nitroxide radicals, traditionally used as biological paramagnetic labels (*13*), such as a narrow single EPR line with minimal hyperfine couplings, and a reduced concentration-dependence of the EPR linewidth (*12*). This makes it possible to dope aqueous samples with relatively large radical concentrations (several tens of mM) and to saturate the EPR spectrum with relatively little RF power. Indeed, in low fields large (negative) Overhauser enhancements have been observed for this radical (−280 in a field of 9.5 mT) (*4, 12*), considerably larger than the enhancements obtained with nitroxide radicals (*2, 14*).

The signal enhancement obtained in OMRI makes the technique potentially useful for increasing the spatial resolution in the images as well, as the NMR sensitivity is one of the key parameters determining this resolution. However, a serious disadvantage of OMRI is that for larger biological objects the experiments have to be performed in low external fields. The reasons for this field limitation are well known. The large dielectric losses in biological samples limit the penetration depth of the RF field and the RF field is partially converted to heat (*15*). Moreover, the DNP enhancement factor decreases with increasing field if the correlation time describing the molecular motions of the water molecules become comparable to or larger than the inverse electron Larmor frequency, $\omega_e^{-1}$ (*7–9*). Therefore, in practice, where biological objects are considered with sizes of a few cm or more, the external fields are usually restricted to 10 mT or less (*3*), which correspond to $\omega_e$ values of 300 MHz or less. This has as a consequence that the overall DNP-enhanced nuclear polarization, which is pro-

[1] To whom correspondence should be addressed. E-mail: robert.wind@pnl.gov.



1090-7807/99 $30.00

portional to the product of both its thermal equilibrium value and the DNP enhancement factor, is not extremely large and can easily be achieved without DNP in a magnet of a moderate field strength, well suited for standard NMR and MRI experiments. Moreover, the NMR sensitivity increases with increasing fields as well, and although this issue can be solved by using field-cycling or sample-shuttling techniques (*2, 3, 16*), where low-field DNP is combined with high-field NMR, it is obvious that low-field DNP in larger samples is hardly useful as a means to increase sensitivity.

The situation is different when DNP is combined with magnetic resonance microscopy (MRM). Here small samples, with sizes of 1 mm or less, need to be used in order to obtain high-resolution images and localized NMR spectra (*17*). This means that the RF frequencies can be made much larger, well into the microwave region, and still have sufficient penetration depth. This follows from the fact that the attenuation of the microwave magnetic and electric fields in a dielectric lossy medium such as water is proportional to $\exp(-s''z)$, where $z$ is the propagation direction and $s''$ is the inverse penetration depth, given by (*18*)

$$(s'')^2 = 0.5\epsilon_o\mu_o\omega^2[\{(\epsilon_r')^2 + (\epsilon_r'')^2\}^{1/2} - \epsilon_r']. \qquad [1]$$

$\epsilon_o$ and $\mu_o$ are the electric permittivity and magnetic permeability in vacuum, respectively, $\epsilon_r'$ and $\epsilon_r''$ are the real and imaginary parts of the relative permittivity of the medium, and $\omega$ is the irradiation frequency. It follows that, e.g., for water at 30°C and $\omega/2\pi = 9$ GHz, where $\epsilon_r' = 66.3$ and $\epsilon_r'' = 25.2$ (*19*), the penetration depth $(s'')^{-1}$ is 3.5 mm. Hence this depth is sufficiently large for DNP MRM applications, and this is true for even larger microwave frequencies as well, provided that the sample size can be made sufficiently small. For instance, the penetration depth in water at 30°C for 40 GHz, where $\epsilon_r' = 21.5$ and $\epsilon_r'' = 30.2$ (*19*), is 0.43 mm (we note that in these examples the effects of the electrical conductivity of water in biological samples, which is on the order of 0.1–1 S $m^{-1}$ (*20*), are neglected. This is justified, because this conductivity causes an increase in $\epsilon_r''$ inversely proportional to $\omega$, and for frequencies in the range 9–40 GHz this increase only produces a minor reduction in the penetration depth). Of course, the sample heating due to the microwave irradiation and the reduction in DNP enhancements at high fields remain serious problems. These issues will be addressed in the next sections.

The purpose of this paper is threefold. First, a DNP NMR setup is described, operating in a field of 1.4 T, in which the microwave heating in small aqueous sample is reduced to acceptable values. Second, the DNP properties of the TAM radical at this field are investigated and evaluated. Finally, the field dependence of the DNP enhancement factor for the TAM radical will be discussed, and the optimal field strength for DNP MRM in aqueous samples will be determined.

As extensive reviews about DNP in liquids have already been published elsewhere (*21, 7–11*), we shall confine ourselves to a brief summary of the main results. In DNP polarization transfer is obtained from the unpaired electron system to the nuclear spin system by saturating the EPR line. This phenomenon is called the Overhauser effect (*6*). The polarization transfer is governed by relaxation transitions, arising from the electron–nuclear scalar and dipolar interactions, rendered time dependent by the molecular motions in the liquids. The resulting Overhauser enhancement factor of the nuclear polarization, $E_{OV}$, is given by

$$E_{OV} = 1 - \rho fsA\gamma_e/\gamma_n. \qquad [2]$$

In Eq. [2], $\rho$ is the coupling factor, determined by the strengths of the electron–nuclear scalar and dipolar interactions and by the spectral density functions characterizing the molecular motions in the liquids; $f$ is the leakage factor, given by $f = R_{II}/(R_o + R_{II})$, where $R_o$ is the nuclear spin–lattice relaxation rate in the absence of the radicals and $R_{II}$ is the nuclear relaxation rate induced by the radicals. Furthermore, s is the saturation factor, given by $s = 1 - M_e/M_{eo}$, where $M_e$ and $M_{eo}$ are the electron polarizations in the presence and absence of the irradiation field, respectively; and $\gamma_e$ and $\gamma_n$ are the electron and nuclear gyromagnetic ratios. Finally, the factor $A$ takes into account the possibility that the EPR spectrum may consist of several lines with such large separations that only part of the spectrum can be saturated. The maximum values of $f$, $s$, and $A$ are unity, whereas in low fields the coupling factor $\rho$ varies between $+1$ for pure scalar interactions and $-1/2$ for pure dipolar interactions, resulting in positive, respectively negative, Overhauser enhancements ($\gamma_e < 0$). It has been found from low-field (9.5 mT) DNP experiments that for the TAM radical in water the scalar interactions can be neglected (*12*). Then $\rho$ is given by

$$\rho = -R_{IS}/R_{II} \qquad [3]$$

$$R_{IS} = (2/3)(\mu_o/4\pi)^2\gamma_e^2\gamma_n^2h^2S(S+1)J(\omega_e) \qquad [4]$$

$$R_{II} = (2/15)(\mu_o/4\pi)^2\gamma_e^2\gamma_n^2h^2S(S+1)\{3J(\omega_n) + 7J(\omega_e)\}. \qquad [5]$$

$\omega_e$ and $\omega_n$ are the electron and proton Larmor frequencies, respectively, and $J(\omega)$ is the spectral density function characterizing the molecular motions. $R_{IS}$ is the mutual electron–nuclear relaxation rate induced by the electron–nuclear dipolar interactions, and $R_{II}$ is the nuclear relaxation rate induced by the radicals. $R_{II}$ is often defined as $cR$, where $c$ is the radical concentration and $R$ the so-called relaxivity of the radical per unit concentration. It follows that $J(\omega)$ determines the frequency dependence of the Overhauser enhancement. Using a model in which the molecules are assumed to be spin-centered, hard spheres without intermolecular forces, the translational diffusion results in a spectral density function given by (*12, 22*)

$$J(\omega) = (cN_A/\pi Db)(3\alpha + 15(\alpha/2)^{1/2} + 12)/ (\alpha^3 + 4\sqrt{2}\alpha^{5/2} + 16\alpha^2 + 27\sqrt{2}\alpha^{3/2} + 81\alpha + 81\sqrt{2}\alpha^{1/2} + 81). \quad [6]$$

$N_A$ is Avogadro's number, $b$ is the minimal distance of approach of a water and radical molecule, $D$ is the sum of the translational diffusion constants of the two molecules, and $\alpha = \omega\tau_c$, where $\tau_c$ is the correlation time, defined as $\tau_c = b^2/D$. We note that a different expression for $J(\omega)$ has been derived using a so-called independent diffusion model (*8, 9*). However, a comparison between the two results revealed that for a frequency range up to 40 GHz the resulting coupling factors differ by no more than 20%. Therefore we confine ourselves to the simple expression for $J(\omega)$, given in Eq. [6]. Also, molecular rotations, arising from either rotations of noncentered spins (*23*) and/or from rotations of complexes of the solvent molecules with the radicals, which can become the dominating motional mechanism for DNP at higher fields in organic solvents (*7–9*), may provide extra contributions to the spectral density function. We shall come back to this matter in the Results and Discussion.

The DNP NMR spectrometer was developed in a collaborative effort between PNNL and the University of Utah and placed at the University. It utilizes a horizontal Magnex magnet with a clear bore size of 22 cm. The magnet operates at a field of 1.4 T, corresponding to electron and $^1$H Larmor frequencies of 40 GHz and 60 MHz, respectively. The NMR part of the spectrometer is a Chemagnetics CMX-100 console. Microwave irradiation is achieved with a Wiltron microwave frequency generator, Model 68263B, and a Traveling Wave Tube amplifier (Logimetrics Model A400/KA), which produces a cw output microwave power of 10 W in the frequency range 26–40 GHz. The probe is home-built, and is a variant of previous designs (*8, 10, 24*). The microwave irradiation is obtained using a combination of a cylindrical horn antenna with a diameter of 10 mm and a movable reflector. This means that the microwaves can penetrate the sample from two directions, and as the penetration depth at 40 GHz is ~0.4–0.5 mm (see above) this allows us to use samples with a width of 0.8–1 mm in the propagation direction of the microwaves. The NMR coil has the same diameter as the horn opening and a length of 15 mm and is placed with its axis coincident with that of the horn antenna. Based upon DNP enhancements observed in nonlossy model solid compounds (*10, 25*), it is estimated that with this design the 10 W incident microwave power corresponds to an amplitude of the (linearly polarized) magnetic component of the microwave field of about 0.1 mT. The probe is equipped with two modulation coils, connected (via a home-built power amplifier) to a SR850 DSP lock-in amplifier from Stanford Research Systems which, in combination with the microwave frequency sweep, makes it possible to perform cw first-derivative 40 GHz EPR. Although its sensitivity is low, this EPR capability is very useful for optimizing both the microwave amplitude and frequency for maximal DNP results.

Without modifications of the DNP probe severe microwave heating of the sample would occur. To estimate the temperature raise that can be expected, we consider the propagation of the microwaves in a water sample with a thickness $d$ in the propagation direction $z$. It can be shown that the rate of energy dissipation per unit volume, $W$, is given by the $z$-derivative of the real part of the Poynting vector $\mathbf{P} = 0.5\,\mathbf{E} \times \mathbf{H}$ (*18*), where $\mathbf{E}$ and $\mathbf{H}$ are the electric and magnetic microwave components. For propagating microwaves in water $|E|$ and $|H|$ are related by $|E| = |Z|\,|H|$, where $|Z|$ is the impedance of water, given by $|Z|^2 = \mu_o/(\epsilon_o|\epsilon_r|)$, with $|\epsilon_r| = [(\epsilon_r')^2 + (\epsilon_r'')^2]^{1/2}$. Then $W$ can be expressed as

$$W = 0.5\omega\epsilon_o\epsilon_r''|E|^2\exp(-2s''z) \quad [\mathrm{W\,m^{-3}}]. \quad [7]$$

The total rate of energy dissipation in the sample, $P$, is found by integrating Eq. [7] over the sample volume $V_s$, and the temperature increase in °C per second, $\Delta T$, is given by

$$\Delta T = 10^{-6}P/(4.184\,V_s) \approx 5.3 \times 10^{-19}\omega\epsilon_r''|E|^2 \times [1 - \exp(-2s''d)]/(s''d) \quad [\mathrm{°C/s}]. \quad [8]$$

As an example we shall consider the effects of microwave irradiation at 40 GHz in a water sample with a thickness $d$ of 1 mm and an initial temperature of 30°C. For the DNP setup used in this investigation, the amplitude of the magnetic component of the microwave field, $|H|$, is maximal about 80 A m$^{-1}$ ($|B| = 0.1$ mT). Using the values $\epsilon_r' = 21.5$ and $\epsilon_r'' = 30.2$ given above, it follows that $s'' \approx 2.3 \times 10^3$ m$^{-1}$, $|Z| \approx 62\ \Omega$, and $|E| \approx 4{,}900$ [V m$^{-1}$]. The result is that $\Delta T \approx 42$°C/s. Hence it takes only a few seconds of microwave irradiation to boil the water, in accordance with experimental observations. To reduce this heating the $E$-field has to be reduced, and to this end special microwave resonators like loop-gap resonators or oversized cavities have been developed, where the $E$-field distribution in the resonator contains nodes where the sample can be placed (*26, 27*). Especially loop-gap resonators have been applied successfully to perform EPR in lossy samples, even for microwave frequencies as high as 35 GHz (*28*), and have also been used for DNP at 9 GHz (*29*). We found that substantial reductions in the $E$-field could also be obtained by winding a solenoid around the sample tube with its axis perpendicular to the $E$-field direction of the microwaves. Figure 1 shows a sketch of the DNP probe with this screening coil in place. It was found that with a proper positioning of the coil and the reflector the microwave magnetic field component was still close to its value obtained without the screening coil, but that the $E$-field, which has nodes at the wire locations, was substantially reduced in the sample as well, resulting in a decreased sample heating. However, it should be noted that these results were found to depend strongly on the positions of

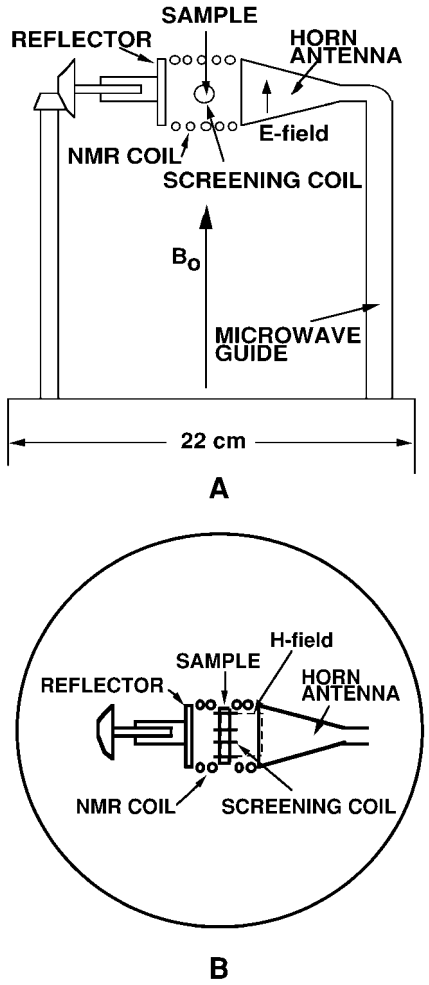


**FIG. 1.** Sketch of the side view (A) and the top view (B) of the DNP NMR probe. The screening coil has a length of 6 mm and consists of 4 turns of 0.6 mm o.d. wire wound tightly around the 1.5 mm o.d. sample capillary. The other parts are explained in the text.

the coil and the reflector and were difficult to reproduce. Therefore, more work is needed to improve the setup. With the screening coil in place the increase in the water temperature was determined after 4 s of microwave irradiation at maximum power (the temperature was determined from the chemical shift change of the water signal, which is given by $-1.33 \times 10^{-2}$ ppm/°C). It was found that for the sample size given below and the screening coil described in the caption of Fig. 1, in the presence of room temperature cooling nitrogen gas around the sample the temperature increase was only 16°C. In fact, for microwave powers of 3 W and below the temperature did not change noticeably. Hence we conclude that the screening coil reduces the *E*-field in the sample by an order of magnitude. It is worth noting that, besides reducing the sample heating, the screening coil has the additional advantage that it can be used to detect NMR as well, thus providing optimal NMR sensitivity (in fact, this setup was used by Wind *et al.* (*24*) for DNP investigations in lossy solids). However, in the present study the large NMR coil was used, mainly because the use of the screening coil would have required a major redesign of the probe layout and because with the existing coil the proton NMR sensitivity was sufficiently large to measure the DNP enhancement factors accurately.

An elaborate description of the TAM radical and its prospects for biological applications has been published elsewhere (*12*). In the present study the symmetric trityl radical was used as described in this reference, the only difference being that our radical was not deuterated. The structure of this radical is given in Fig. 2. For our investigations 10 mM of this radical was dissolved in deionized water. The sample was poured into a capillary with an o.d. of 1.5 mm, an i.d. of 1 mm, and a length of 6 mm, after which the capillary was sealed. The sample was not degassed, which allowed us to determine the saturation properties of the radical at 1.4 T in a biologically more realistic case of oxygen containing water.

All measurements were carried out at 26°C. In (*12*) the correlation time $\tau_c = b^2/D$, governing the DNP effect, was determined at 23°C, using a minimal distance of approach of a water and radical molecule, $b$, of $5.45 \times 10^{-10}$ m, and approximating $D$ by the diffusion coefficient of free water, $D = 1.9 \times 10^{-9}$ m$^2$/s. The result is that $\tau_c = 156 \pm 13$ ps. Using this value and using the activation energy of the diffusion coefficient in water of 4.9 kcal/mol (*30*), it can easily be calculated that at 26°C this correlation time is given by $143 \pm 13$ ps. This value will be used to evaluate the 1.4 T DNP results.

Figure 3A shows the EPR spectrum of the TAM radical, measured in an external field of 10 mT in a degassed sample. As reported before (*12*), for this type of radicals the spectrum consists of a narrow central linewidth a width of 6 $\mu$T and an array of ten (partially degenerate) $^{13}$C satellite lines. The centers of these lines do not coincide with the central line. This is a result of second-order hyperfine splittings which become pronounced in this low field (*31*). For instance, the center of the outer two lines, which are separated by 31 MHz, is shifted 0.9 MHz downfield relative to the center line. It has been determined in (*12*) that the presence of the satellites reduces the factor $A$ in Eq. [2] to 0.89, and this number shall be used in the analysis of the DNP results. With the insensitive 40 GHz EPR setup used in our measurements only the central line could be detected (however, the satellite lines could clearly be observed

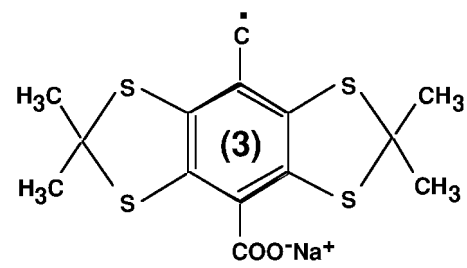


**FIG. 2.** The molecular structure of the symmetric trityl radical.

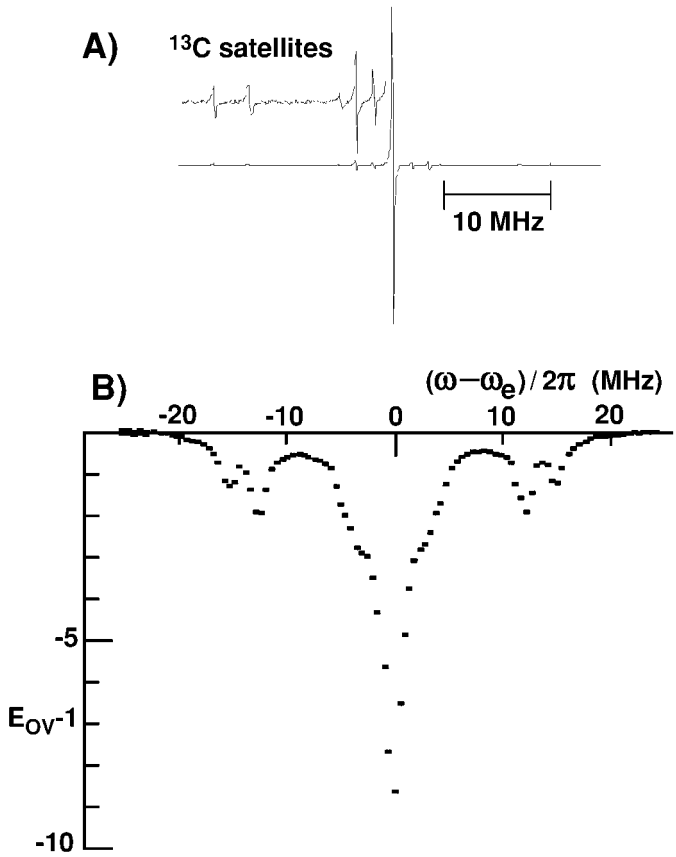


**FIG. 3.** (A) The EPR spectrum of the symmetric trityl radical dissolved in degassed water. The spectrum was measured in an external magnetic field of 10 mT. (B) The $^1$H Overhauser enhancement $E_{OV}$ as a function of the microwave off-set frequency ($\omega - \omega_e$) and an incident microwave power of 9 W. The microwave frequency was swept in steps of 0.5 MHz over a range of 50 MHz. The enhancement curve reflects the saturated EPR spectrum.

in the DNP enhancement curve, given in Fig. 3B). It was found that in the nondegassed sample the presence of the oxygen increased the width of this line to 21 $\mu$T.

The proton spin–lattice relaxation times in the absence and presence of the radical were found to be 2.44 s and 0.90 s, respectively. It follows from this result that the leakage factor $f$ is 0.63 and that the relaxivity $R = R_{1H}/c$ of the TAM radical at 60 MHz is 0.070 $(\text{mMs})^{-1}$. This corresponds to a low-field relaxivity of 0.21 $(\text{mMs})^{-1}$, taking into account that $\omega_e\tau_c \gg 1$ at 1.4 T, and hence $J(\omega_e) \ll J(\omega_n) \approx J(0)$, which reduces $R$ to 0.3 times its low-field value, cf. Eq. [5]. This low-field value is in accordance with experimental results observed in fields of 10 mT and smaller (*12*).

Figure 3B shows the DNP enhancement curve, i.e., the $^1$H Overhauser enhancement factor as a function of the microwave frequency. This curve reflects the (saturated) EPR spectrum, which resembles closely the low-field EPR spectrum, except for the increased linewidths as a result of the presence of oxygen and the microwave irradiation, and for the second-order hyperfine splittings, which become negligibly small at 1.4 T. It follows from Fig. 3B that the proton Overhauser enhancement is negative, indicating that also at higher fields the dipolar electron–nuclear interactions are the dominant DNP mechanisms. The coupling factor $\rho$ can be determined from Eq. [2], provided that $f$, $s$, and $A$ are known. It has already been established above that $f = 0.63$, and $A = 0.89$, so that the only parameter left is the saturation factor $s$. The usual way to determine this factor is measuring the enhancement $(E_{OV} - 1)$ as a function of the microwave power. If the microwave field is homogeneously distributed over the sample, the saturation factor can be expressed as $s = \beta P_e/(1 + \beta P_e)$, where $\beta$ is a constant and $P_e$ is the microwave power. In this case the parameter $(E_{OV} - 1)^{-1}$ should be linearly proportional to $(P_e)^{-1}$, cf. Eq. [2], so that extrapolation of the plot $(E_{OV} - 1)^{-1}$ versus $(P_e)^{-1}$ to zero $(P_e)^{-1}$ provides the enhancement factor for $s = 1$. The experimental plot is given in Fig. 4. Here the Overhauser enhancement was determined as a function of power after a 4 s microwave irradiation, which is sufficiently long for the nuclear polarization to reach its stationary value. It follows that for larger values of $(P_e)^{-1}$ indeed a linear relationship is observed. For smaller $(P_e)^{-1}$ values $(E_{OV} - 1)^{-1}$ decreases nonlinearly with $(P_e)^{-1}$, resulting in increased enhancement factors for larger microwave powers than follow from extrapolation of the low-power results. This is mainly due to the temperature increase in the sample at elevated micro-

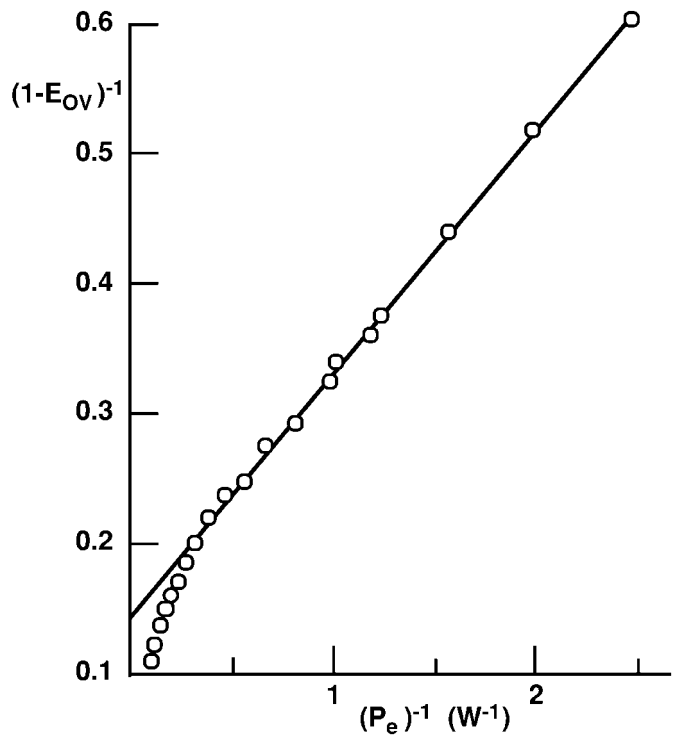


**FIG. 4.** The inverse Overhauser enhancement, $(1 - E_{OV})^{-1}$, as a function of the inverse microwave power $P_e^{-1}$, where $P_e$ denotes the incident microwave power in W. Open circles: experimental; solid line: linear dependence between $(1 - E_{OV})^{-1}$ and $P_e^{-1}$, determined from the low-power results.

wave powers. The chemical shift value of the water line revealed that for $(P_e)^{-1} > 0.3$ W$^{-1}$ no noticeable temperature change occurred, and that for $0.1 < (P_e)^{-1} < 0.3$ W$^{-1}$ the temperature gradually increased from 26 to 42°C at maximum power. This temperature increase causes a decrease in the correlation time and, therefore, an increase in DNP enhancement, and indeed the enhancement increase measured for larger microwave powers is consistent with the sample temperature (we note that this nonlinearity can also be caused by an inhomogeneous microwave field distribution over the sample, resulting, e.g., from the finite penetration depth of the microwaves and the presence of the screening coil. Then the inverse saturation factor is no longer proportional to $P_e{}^{-1}$, and the relationship between $(P_e)^{-1}$ and $(E_{OV} - 1)^{-1}$ becomes nonlinear. However, this inhomogeneity is probably not that large, as during the 4 s of microwave irradiation much of the sample will be submitted to a same average microwave field as a result of microscopic and macroscopic thermal motions in the water. Therefore the effects of this inhomogeneity will be neglected).

Extrapolating the linear part of the $(P_e)^{-1}$ versus $(E_{OV} - 1)^{-1}$ curve, observed for $(P_e)^{-1} > 0.3$, to $(P_e)^{-1} = 0$, it follows from Fig. 4 that $(E_{OV} - 1)^{-1} = -0.145$ ($E_{OV} - 1 = -6.9$) for infinite microwave power, i.e., $s = 1$. It also follows from this plot that the saturation factor at maximum power is large, $s = 0.89$. Using this value, and approximating $s$ by $s \approx \gamma_e{}^2 B_1{}^2 T_{1e} T_{2e}/(1 + \gamma_e{}^2 B_1{}^2 T_{1e} T_{2e})$, the average amplitude of the magnetic component of the microwave field can be estimated ($T_{1e}$ and $T_{2e}$ are the electron spin–lattice and spin–spin relaxation times). It follows from the unsaturated EPR spectrum that $T_{2e} = 320$ nsec, and it is estimated that in oxygen-containing water $T_{1e}$ is about $1.5T_{2e} = 480$ nsec (*12*). Using these values it follows that $B_1 = 0.04$ mT at maximum power. Hence the linearly polarized microwave field is 0.08 mT, comparable to the value of 0.1 mT, estimated from DNP experiments in nonlossy solids, see above. We conclude that the screening coil only induces a minor decrease in the $B$-field of the microwaves. Finally, it follows from Fig. 4 that for $(P_e)^{-1} = 0.3$, where $E_{OV} - 1 = -5.0$, the saturation factor is 0.73. This means that even at reduced microwave powers, where the sample heating can be neglected, still relatively large saturation factors are obtained.

Using the values $E_{OV} - 1 = -6.9$ for $s = 1$, $f = 0.63$, and $A = 0.89$, it follows from Eq. [2] that the Overhauser enhancement for $s = f = A = 1$ becomes given by $-12.3$, corresponding to a coupling factor $\rho$ at an electron Larmor frequency of 40 GHz of $-0.0187$. Using the correlation time of $143 \pm 13$ ps, it follows that Eqs. [3–6] predict a coupling factor of $-0.0193 \pm 0.0025$, in excellent agreement with the experimental value. This can also be observed in Fig. 5, where the frequency dependence of $\rho$ is given. In this figure also the low-field coupling factor is given reported in (*12*). We also evaluated the effects of the eccentricity of the water molecules on the spectral density function (*23*). It was found that inclusion of this model resulted in marginal corrections for the coupling factor, with a tendency to overestimate its value. Moreover, it can be remarked that the formation of rotating solvent-radical complexes is not apparent for the TAM radical in water. Therefore we conclude that for all frequencies the Overhauser effect is governed by electron–nuclear dipolar interactions only, and that the time dependence in the relaxation transitions is determined by the translational diffusion of the water molecules.

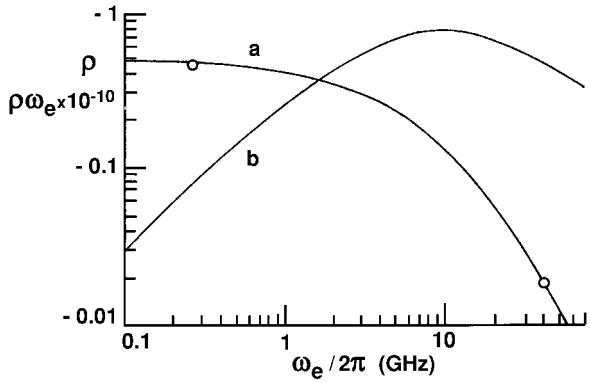


**FIG. 5.** The coupling factor $\rho$ (curve a) and the product of $\rho$ and the electron Larmor frequency $\omega_e$ (curve b) as a function of $\omega_e$. The coupling factor has been calculated from Eqs. [3]–[6], using a correlation time of 143 ps. Open circles: experimental. The low frequency value of $\rho$ is obtained from Ref. (*12*).

Finally, in Fig. 5 also the product $\rho\omega_e$, which is a measure for the overall enhanced nuclear polarization, is given. It follows that this value becomes maximal for $\omega_e \approx 9$ GHz. This means that the standard EPR frequency of 9 GHz is an excellent choice for DNP MRM, also because at this frequency the microwave penetration depth is still a few mm, very acceptable for MRM research, and because the optimal frequency increases only slowly with temperature (e.g., at 37°C this frequency becomes 12 GHz).

It has been shown that with a relatively simple DNP device, consisting of a horn antenna, a reflector, and a coil closely wound around the sample capillary tube, it is possible to perform DNP on aqueous samples at 1.4 T without excessive sample heating. In fact, incident microwave powers up to 3 W, corresponding to an amplitude of the (linearly polarized) magnetic component of the microwave field of about 0.04 mT, could be applied for at least 4 s without any noticeable increase in the sample temperature. It should be emphasized that, as so far no attempts have been made to optimize this design, it is likely that its performance can be further improved. This will be explored in future investigations, which will also include DNP MRM to map the Overhauser enhancement distribution over the sample.

It was found that, like in low fields, in the relatively large external field of 1.4 T the TAM radical has favorable DNP properties. Even in oxygenated water the EPR line is easy to saturate, which compares favorably with nitroxide radicals,

where in our setup no DNP enhancement was observed under these conditions. Moreover, large radical concentrations can be used, so that the leakage factor can be made rather large, even in biological samples where the relaxation time of the water protons in absence of the radicals is reduced, or in larger fields where the relaxivity of the radical is reduced. It was determined that at 1.4 T the spectral density function, governing the radical-induced relaxation transitions, is completely determined by translational diffusion, which means that the contributions of rotating noncentered spins or rotating radical–water complexes can be neglected. This result is in contrast to DNP at this field in organic liquids, where it has been found that rotations of radical–solvent complexes can become the dominating motional mechanism (*7–9*).

With respect to the possible application of DNP for MRM the following can be remarked. For the TAM radical dissolved in water it was determined that the DNP-enhanced polarization should become maximal in a field of about 0.3 T. At this field a maximum (i.e., for $s = f = A = 1$) DNP enhancement of about 92 is expected at 26°C, and this can be further increased if the temperature can be raised (for instance, at 37°C the enhancement becomes 50% larger). This means that at 26°C the DNP-enhanced polarization in this field equals the thermal equilibrium polarization in a field of 29 T, which is considerably larger than the largest available high-resolution magnet field available to date. Therefore, we think that the DNP MRM in medium field strengths has the potential of improving the MRM capabilities, so that images can be obtained with larger spatial resolutions than is possible at present. Moreover, additional advantages of using medium fields are that the influence of sample losses on the NMR sensitivity becomes negligibly small, and that susceptibility broadenings in the sample, which arise in samples containing porous media and cause signal losses and image distortions in large fields (*17*), are reduced.

We finally note that the utility of the TAM radical for DNP MRM may be further increased if this type of radical can also be dissolved in nonlossy liquids or supercritical fluids. In these solvents the correlation times can be considerably smaller than in water, resulting in increased enhancement factors at higher fields. In fact, under these conditions a field of 1.4 T or even higher may become the field of choice for DNP MRM. It is expected that a simple chemical modification in the *para* position of the aromatic parts of the radical such as estherification will result in radicals that can be used in these types of solvents, and which possess similar magnetic resonance properties as the TAM radical considered in this paper.

## ACKNOWLEDGMENTS

The authors thank Professors D.M. Grant and R.E. Pugmire of the University of Utah for permitting the use of their research facility at the University, Drs. J. Z. Hu and M. S. Solum of the University of Utah for their assistance with the experiments, and Dr. K. R. Minard of the Pacific Northwest National Laboratory for assistance with the evaluation of the microwave-induced losses. The work was supported by the Pacific Northwest National Laboratory, a multiprogram laboratory operated by Battelle Memorial Institute for the U.S. Department of Energy under Contract DE-AC06-76RLO 1830.

## REFERENCES

1. D. J. Lurie, D. M. Bussell, L. H. Bell, and J. R. Mallard, Proton-electron double magnetic resonance imaging of free radical solutions, *J. Magn. Reson.* **76,** 366–370 (1988).
2. D. J. Lurie, J. M. S. Hutchison, L. H. Bell, I. Nicholson, D. M. Bussell, and J. R. Mallard, Field-cycled proton-electron double-resonance imaging of free radicals in large aqueous samples, *J. Magn. Reson.* **84,** 431–437 (1989).
3. H. Konijnenburg and A. F. Mehlkopf, Optimal field strength and pulse-sequence parameters for *in vivo* dynamic-polarization imaging, *J. Magn. Reson.* **B113,** 53–58 (1996).
4. H. Konijnenburg, J. Trommel, J. H. Ardenkjaer-Larsen, and A. F. Mehlkopf, Functional Overhauser imaging and functional MRI: A comparison, *in* "Proceedings: ISMRM Fifth Scientific Meeting, Vancouver, BC, Canada," p. 2129.
5. P. Kuppusamy, P. Wang, M. Chzhan, and J. L. Zweier, High resolution electron paramagnetic resonance imaging of biological samples with a single line paramagnetic label, *MRM* **37,** 479–483 (1997).
6. A. W. Overhauser, Polarization of nuclei in metals, *Phys. Rev.* **92,** 411–415 (1953).
7. K. H. Hausser and D. Stehlik, Dynamic nuclear polarization in liquids, *in* "Advances in Magnetic Resonance" (J.S. Waugh, Ed.), Vol.3, pp 79–139, Academic Press, New York (1968).
8. J. Trommel, "Molecular Motions and Collisions in Organic Free Radical Solutions as Studied by Dynamic Nuclear Polarization," Thesis, Delft University of Technology, Delft, The Netherlands (1978).
9. W. Müller-Warmuth and K. Meise-Gresch, Molecular motions and interactions as studied by dynamic nuclear polarization (DNP) in free radical solutions, *in* "Advances in Magnetic Resonance" (J. S. Waugh, Ed.), Vol. 11, pp. 1–45, Academic Press, New York (1983).
10. R. A. Wind, M. J. Duijvestijn, C. van der Lugt, A. Manenschijn, and J. Vriend, Applications of dynamic nuclear polarization in $^{13}C$ NMR in solids, *Progr. in NMR Spectr.* **17,** 33–67 (1985).
11. R. D. Bates, Jr, Dynamic nuclear polarization, *Magn. Reson. Review* **16,** 237–291 (1993).
12. J. H. Ardenkjaer-Larsen, I. Laursen, I. Leunbach, G. Ehnholm, L.-G. Wistrand, J. S. Petersson, and K. Golman, EPR and DNP properties of certain novel single electron contrast agents intended for oximetric imaging, *J. Magn. Reson.* **133,** 1–12 (1998).
13. D. Marsh, Recent developments in spin labeling, *in* "Bioradicals Detected by ESR Spectroscopy" (H. Ohya-Nishiguchi and L. Packer, Eds.), pp. 173–191, Birkhauser Verlag, Basel (1995).
14. D. Grucker, T. Guiberteau, B. Eclancher, J. Chambron, R. Chiarelli, A. Rassat, G. Subra, and B. Gallez, Dynamic nuclear polarization with nitroxides dissolved in biological fluids, *J. Magn. Reson. B* **106,** 101–109 (1995).
15. H. M. Swartz and T. Walczak, *In vivo* EPR: prospects for the '90s, *Physica Medica* **9,** 41–48 (1993).
16. H. C. Dorn, R. Gitti, K. H. Tsai, and T. E. Glass, The flow transfer of a bolus with $^{1}H$ dynamic nuclear polarization from low to high magnetic fields, *Chem. Phys. Lett.* **155,** 227–232 (1989).
17. P. T. Callaghan, "Principles of Nuclear Magnetic Resonance Microscopy," Clarendon Press, Oxford (1993).

*18.* J. R. Christman, "Fundamentals of Solid State Physics," Wiley, New York (1988).

*19.* U. Kaatze and V. Uhlendorf, The dielectric properties of water at microwave frequencies, *Z. Fur Physikal. Chemie Neue Folge* **126,** 151–165 (1981).

*20.* S. Gabriel, R. W. Lau, and C. Gabriel, The dielectric properties of biological tissues: III. Paramagnetic models for the dielectric spectrum of tissues, *Phys. Med. Biol.* **41,** 2271–2293 (1996).

*21.* A. Abragam, "The Principles of Nuclear Magnetism," Clarendon Press, Oxford (1961).

*22.* Y. Ayant, E. Belorizky, J. Alizon, and J. Gallice, Calcul des densités spectrales résultant d'un mouvement aléatoire de translation en relaxation par interaction dipolaire magnétique dans les liquides, *Le Journal de Physique* **36,** 991–1004 (1975).

*23.* Y. Ayant, E. Belorizky, P. Fries, and J. Rosset, Effet des interactions dipolaires magnétique intermoléculaires sur la relaxation nucléaire de molecules polyatomiques dans les liquides, *Le Journal de Physique* **38,** 325–337 (1977).

*24.* R. A. Wind, F. E. Anthonio, M. J. Duijvestijn, J. Smidt, J. Trommel, and G. M. C. de Vette, Experimental setup for enhanced $^{13}C$ NMR spectroscopy in solids using dynamic nuclear polarization, *J. Magn. Reson.* **52,** 424–434 (1983).

*25.* M. J. Duijvestijn, R. A. Wind, and J. Smidt, A quantitative investigation of the dynamic nuclear polarization effect by fixed paramagnetic centers of abundant and rare spins in solids at room temperature, *Physica B* **138,** 157–170 (1986).

*26.* W. Froncisz and J. S. Hyde, The loop-gap resonator: A new microwave lumped circuit ESR sample structure, *J. Magn. Reson.* **47,** 515–521 (1982).

*27.* J. S. Hyde, W. Froncisz, and T. Oles, Multipurpose loop-gap resonator, *J. Magn. Reson.* **82,** 223–230 (1989).

*28.* W. Froncisz, T. Oles, and J. S. Hyde, Q-band loop-gap resonator, *Rev. Sci. Instr.* **57,** 1095–1099 (1986).

*29.* P. Dirksen, J. A. J. M. Disselhorst, H. van der Meer, and W. Th. Wenckebach, A loop-gap resonator for microwave-induced optical nuclear polarization, electron spin-echo experiments, and dynamic nuclear polarization, *J. Magn. Reson.* **87,** 516–522 (1990).

*30.* D. C. Chang, H. E. Rorschach, B. L. Nichols, and C. F. Hazlewood, Implications of diffusion coefficient measurements for the structure of cellular water, *Ann. NY Acad. Sci.* **204,** 434–443 (1973).

*31.* J. E. Wertz and J. R. Bolton, "Electron Spin Resonance," Chapman and Hall, New York (1986).